RESEARCH PROJECT IN MECHANICAL ENGINEERING

Balancing the printability and final performance of nanocomposite conductive inkjet inks

Devdass Krishnan

Project Report ME063-2019

Co-worker: Ryan Welsh

Supervisor: Dr Jonathan Stringer

Department of Mechanical Engineering
The University of Auckland

20 May 2021

Balancing the printability and final performance of nanocomposite conductive inkjet inks

Devdass Krishnan

ABSTRACT

An investigation into the printability and final performance of a set of bio-based carbon fibre conductive inkjet inks was performed. Triton X-100 and various concentrations of glycol is used to influence the dispersion of carbon fibre throughout the ink, and the shelf life of the ink. These additives were also used to influence the surface profile and resistivity of printed samples. The optimal concentration of glycol was found to be 10.09%. Ink containing glycol at this level was found to have to most consistent distribution of carbon fibre throughout printed shapes, improved shelf life, significantly improved surface profile uniformity, and has relatively low resistance. Samples were treated in a plasma oven to remove impurities. Using a four point probe, it was found that the resistance of these treated samples had decreased by a factor of 10,000.

Table of Contents

List of Tables

List of Figures

1. Introduction

In a world where electronics are becoming much cheaper to manufacture, it is important to consider the end of life of these electronics and what impact that they may have on the environment.

An ever decreasing cost makes it more viable to develop disposable electronics which encourages more packaging manufactures to embed disposable electronics into their products. Embedded sensors in packing unlocks the opportunity for automatic tracking of parcels through supply chains, checkout-less supermarkets, environmental monitoring of perishables such as food or pharmaceuticals, and other novel applications. An example of a current use case for disposable electronics can be seen behind the cover of library books in the form of an RFID tag to prevent theft [1].

Studies based on carbon based conductive inkjet inks have shown potential for these materials to be used in the manufacture of flexible electronics. The investigation concerns a bio-based alternative to metal for the use in flexible, printable, and disposable electronics. An experiment is conducted in order to further characterise and optimise inkjet inks containing the conductive bio-based material, for printing in the manufacture of the aforementioned electronics.

However, many of these studies struggle to detail the ways in which the production and use of these materials can be environmentally sustainable. Almost all disposable electronics are sent to landfills when they're no longer used or reach their end of life. Generally, it is difficult or cost-inefficient to recover the metals used in these electronics, so many recyclers do not bother to do so. Many of these studies struggle to detail the ways in which the production and use of these materials can be environmentally sustainable..

This is partly due to the ways the carbon material is manufactured, and it is also due to the methods in which the fluid is optimised to enable reliable printability. This study investigates how lignin, what was once seen as a waste material, can be used to sustainably produce carbon fibres for the use in conductive inkjet inks. This report discusses the issues faced when balancing ideal ink characteristics with printability.

1.1 Literature

Printed electronics are part of a growing trend of interest in the scientific community. They show potential to be used in a wide variety of applications such as transistors [2], flexible displays [3], antennas [4], flexible batteries [5], and sensors [1]. Various forms of additive manufacturing (AM) exist that have been used for the production of these electronics. Such AM processes include; 3D printing, inkjet printing, laser sintering, air-brush spraying, dip-pen nanolithography, slot-dye coating, gravure printing, and extrusion printing [6].

1.1.1 Carbon-based Inks

Carbon is a material that is often used in these studies. Carbon materials are investigated for their great thermal and electrical conductive properties. Carbon nanofibres (CNFs) and carbon nanotubes (CNTs) are the dominant areas of focus for those involved in conductive carbon technologies related to the manufacture of electronics [6–11]. CNT and CNF based inks rely on a network of interconnecting particles to carry current across the ink. Some studies concerning conducting carbon technologies have focused on deposition techniques [6, 10, 12], dispersion optimisation [6, 11], composites [9], and material precursors [13].

1.1.2 Lignin

Lignin is one of the worlds most copious bio-based renewable resources. It can also be used to produced low cost carbon fibres via the melt spinning process [14]. The New Zealand Ministry for Primary Industries reports NZ relies on forestry for 3% of its total GDP and is the third biggest earning export. Lignin is obtained as a byproduct from the wood pulping process and is burned for use in industrial heating. Unfortunately, heating by combustion is much cheaper compared to electrical heating, which significantly contributes to climate change. This study aims to support the growing interest in providing bio-based alternatives for fossil-based high-performance materials [13], giving value to lignin, which was once seen as a waste product.

1.1.3 Dispersion and Agglomeration

Many of the aforementioned studies report difficulties concerning the homogeneous dispersion of their respective carbon suspensions. This lack of natural solubility, known as agglomeration, is attributed to the hydrophobic structure of CNFs and CNTs. Agglomeration issues have been known to clog orifices used in AM, hindering production [8]. For the purpose of this investigation, this study adopts some of the techniques demonstrated within those studies to counter agglomeration.

2. Experimental

2.1 Carbon Fibre Solutions

Six inks are featured in this project. They were supplied by Scion, a Crown research institute. They are named as follows: RA-013-1a, RA-013-2a, RA-013-3a, RA-011-1a, RA-011-2a, and RA-011-3a. Each ink contained a carbon fibre concentration of 1.7%. The RA-011 series of inks contained 0.1% nanocellulose whereas the RA-013 series of inks contained no nanocellulose. The 1a, 2a, and 3a suffix refers to 0.7%, 1.0%, and 1.2% concentrations of protein within the respective inks.

Solution Name	Nanocellulose Concentration (%)	Protein Concentration (%)
RA-011-1a	0.1	0.7
RA-011-2a	0.1	1.0
RA-011-3a	0.1	1.2
RA-013-1a	0	0.7
RA-013-2a	0	1.0
RA-013-3a	0	1.2

Table 1 Ink Compositions

2.2 Inital Characterisation

2.2.1 Preliminary Viscosity Testing

To gain an inital understanding of the qualities of each ink solution, viscocity tests were conducted using a Brookfield DV3T viscometer. At this point, it became apparent that the RA-011 series of inks were significantly more viscous compared to the RA-013 series of inks. Proceeding these viscosity tests it was recommended that a solution with an average viscosity value closest to $10mPa \cdot s$ is chosen; RA-013-1A was selected for further testing. Due to time constraints, resources were allocated towards further testing of the RA-013 series.

Figure 1   Brookfield DV3T viscometer

Soulution	Viscocity $(mPa \cdot s)$
RA-011-1A	53.37
RA-011-2A	37.79
RA-011-3A	15.84
RA-013-1A	7.425
RA-013-2A	2.005
RA-013-3A	1.993

Table 2   Average Viscocity Values (pre-treatment)

2.2.2   Initial Print

Using solution RA-013-1A, test prints were made. The printer used in the investigation was an experimental inkjet printer with an MJ-ATP-01 drop-on-demand single jet dispensing print head device from Microfab Technologies. Prior to loading the solution into the printer reservoir, it was sonicated in a water bath for 30 minutes. This is to break up any aggregate carbon fibres that may have collected while in storage. If carbon fibre agglomeration is prevalent enough, the entangled structures may block the 60 micron print head orifice, disabling the printer until the blockage is cleared.

Initially, films were printed using RA-013-1A at a droplet dispensing frequency of 200Hz. Using a 2D motorised print bed, shapes were printed after uploading the appropriate G-code to the controller. The chosen shape was a 1.2cm x 1.2cm square. Only partial success was achieved with this combination of solution and frequency as intermittent printing issues were encountered, as shown in figure 3. This is attributed mainly to the clogging of the print head orifice caused by agglomeration, despite the initial 30 minutes of sonication. Following this, the dispensing frequency was increased from 200Hz to 500Hz so that if there are parts of the printed shape that are incomplete, the increased amount of liquid on the substrate will be able to cover it. An increase in frequency of printing issues was encountered, also attributed to a clogged print orifice. To avoid this issue, the print head was flushed with DI water to remove any aggregated carbon fibres and had also further sonicated the solution using a Sonics Vibra-Cell ultrasonic liquid processor. The results of these efforts are shown in figure 4. These results were worse than that of 200Hz.
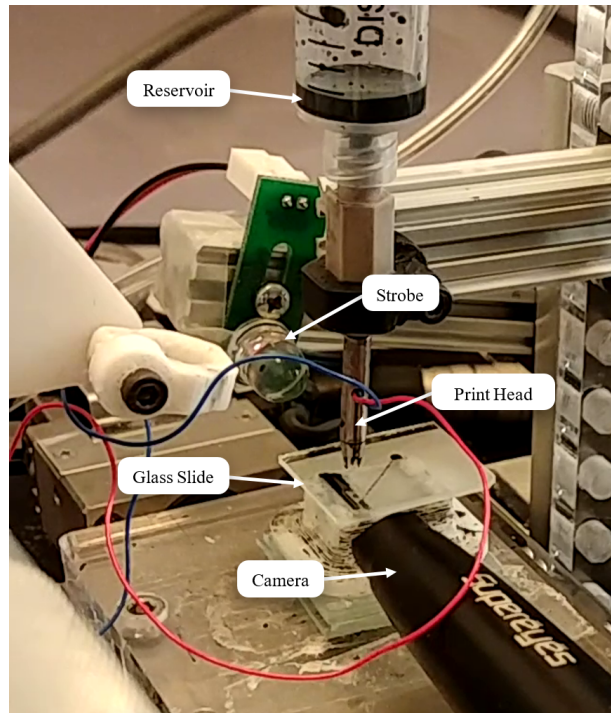
Figure 2   Inkjet Printer Diagram

Figure 3   RA-013-1A Print at 200Hz (no additives)
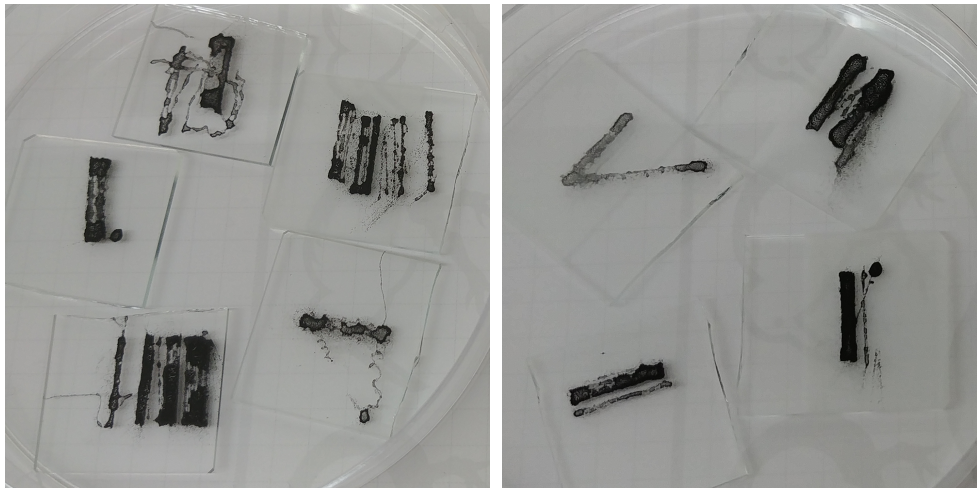
(a)   (b)

Figure 4   RA-013-1A Print at 500Hz (no additives)

2.3 Agglomeration and Treatment

2.3.1 Triton X-100

Clearly, sonication did not have any significant effect on the prevalence of agglomeration on the original RA-013-1A formulation. Acting on the advice of existing literature [11,15], it was decided to use a surfactant known as Triton X-100 to counter agglomeration as it is known to be very effective in dispersing carbon nano-materials. Triton X-100 was added to the RA-013-1A solution - this solution is named RA-013-1A'. The net weight percentage of surfactant in the RA-013-1A' was 1%. Sonication had created many bubbles within the RA-013-1A' solution so it was left to settle overnight. Upon returning, a print was produced using RA-013-1A' without sonication prior to printing. The results are as shown in figure 5. This print took longer to dry than that of the unmodified solution prints in figure 4. The higher water content suggests that while the RA-013-1A' solution was left to
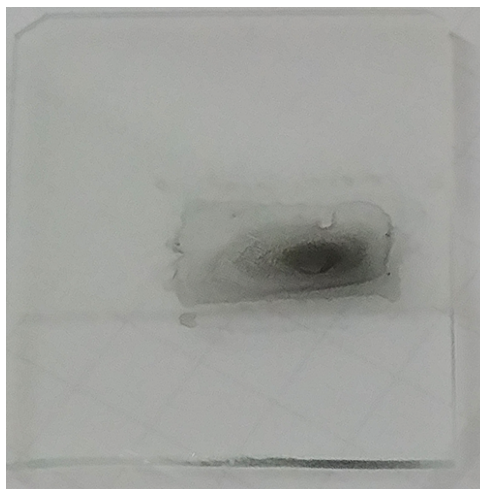
Figure 5   RA-013-1A + Triton X-100 Print at 500Hz (24hrs without sonication)

settle overnight, some of the carbon fibres had sunken to the bottom of its container - as a result, the fluid reservoir didn't contain as many carbon fibres. The RA-013-1A' solution was then sonicated in a water bath for 30 minutes and under an ultrasonic liquid processor
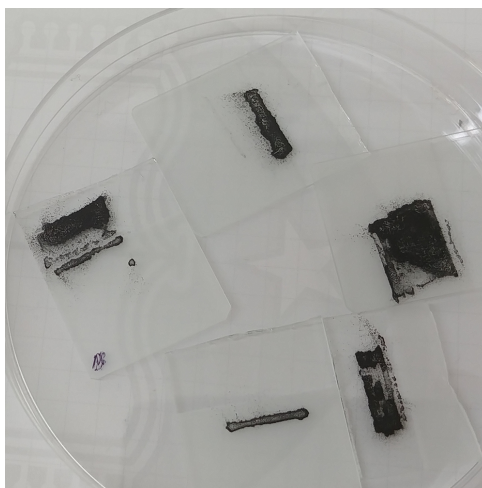
Figure 6 RA-013-1A + Triton X-100 Print at 500Hz (with sonication)

Figure 7 RA-013-1A Hand-laid droplets

for 60 seconds. The sonicated RA-013-1A' solution was now printing with better results, as shown in figure 6, compared to that of the unmodified solution in figure 4. Intermittent blockage was still an occurrence, however, the coating of the glass slide substrate was more even. The prints made with RA-013-1A' became progressively worse as more of the solution was used. Intermittent print head orifice blocking became more frequent. It is suspected that most of the fluid's water content that contained sufficiently dispersed carbon fibres. The fluid that remained had a higher concentration of particulates, and therefore was more prone to agglomeration. At this point, the decision was made to suspend further investigation of RA-013-1A and RA-013-1A'.

2.4 Coffee Ring Effect

The coffee ring effect is the name given to a phenomenon that results in a ring-like deposit of particles after the liquid containing those particles evaporates, similar to that of coffee stains. This phenomenon is visible in some of the early hand-laid droplet samples of RA-013-1A, as seen in figure 7. This effect is undesirable as it reduces the resistivity of the printed shapes. This is caused by a reduced concentration of interconnecting carbon fibres that carry current across the entire printed shape. However this effect is desired by some in the manufacture of transparent conductive films [16] because light can pass through most of the dispensed droplet whilst remaining conductive through its edge.

2.4.1 Glycol

What researchers have done before to counteract this effect, is to add the surfactant-like organic compound; ethylene glycol to the working solution [17, 18]. Ethylene glycol

Sample Number (#)	1	2	3	4	5	6
Glycol Weight (g)	0.0000	0.2571	0.5053	0.7538	1.0030	1.2616
RA-013-2A' Weight (g)	4.9951	5.0143	5.0077	5.0055	5.0152	5.0038
Glycol Concentration (%)	0.0000	5.1273	10.0905	15.0594	19.9992	25.2128

Table 3   RA-013-2A samples with Triton X-100 and varying Glycol concentrations

(a)   (b)   (c)
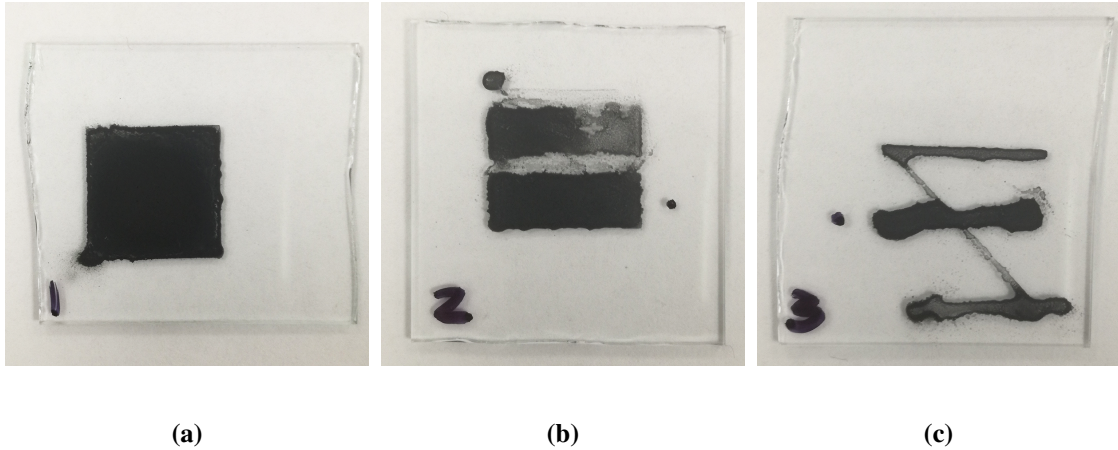
Figure 8   RA-013-3A with glycol and Triton X-100 Print at 500Hz

modifies the surface tension of the solution, increasing the energy requirement for fluid particles to evaporate.

To investigate the effect glycol has on the inks, varying amounts of glycol was added to the RA-013-2A solution after dividing it into six different samples and also adding Triton X-100 to the solution which amounted to 1% of its total weight. RA-013-2A was chosen because there wasn't a sufficient amount of RA-013-3A left to use and RA-013-1A was no longer in its original condition after using it repeatedly in this study. Before being divided, the base RA-013-2A solution containing Triton X-100 is named RA-013-2A'. The concentrations of the aforementioned samples are detailed in table 3.

2.4.2   Stability Test

Prior to creating the glycol solutions in table 3, glycol and Triton X-100 was added to RA-013-3A. The glycol amounted to 1% of the total solution weight, as did the Triton X-100. This solution was created to observe the effect of shelf time on the stability of the ink. In other words, it is important to see whether the solution was still functional without the need for sonication after an extended period of time in storage.

An attempt was made to print the RA-013-3A solution with glycol and Triton X-100 after sonicating it for 30 minutes in a water bath and for 1.5 minutes under the ultrasonic liquid processor. Successful was achieved in printing a complete square using this solution, as shown in figure 8a. However, the maintenance of this success was not achieved as the print head orifice would clog.

A period of four days had elapsed before another attempt was made to print again using the same solution, without sonicating it prior to printing. These prints, as shown in figure 9, are less dense than those in figure 8. This is due to sedimentation of the carbon fibres in the solution's storage container. However, the printed shape is spread more evenly. This is probably due to the higher water content of the print.

(a)   **(b)**   **(c)**
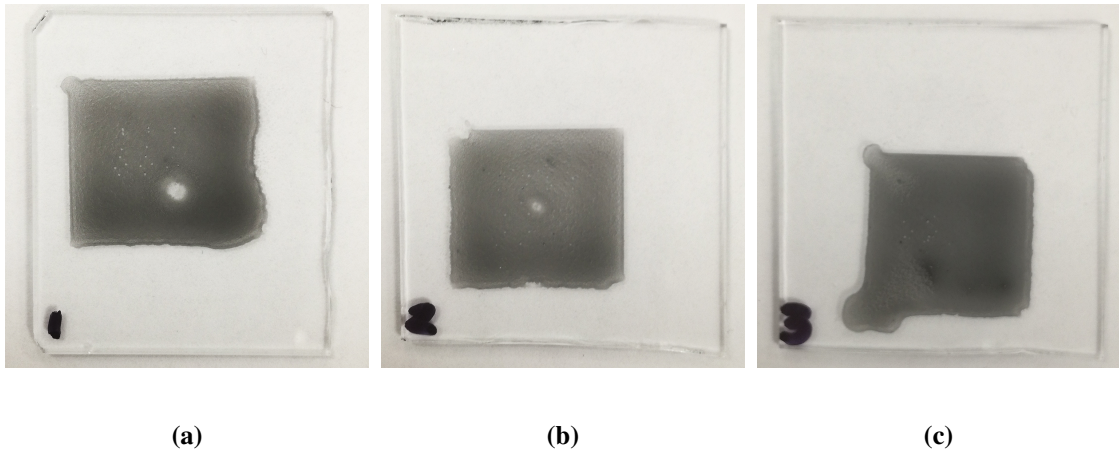
Figure 9   RA-013-3A with glycol and Triton X-100 after 4 days of storage Print at 500Hz

Generally, attempting to print films using any of the solutions that contained glycol produced results better than the prints that did not contain glycol. Some of the glycol prints have a more consistent distribution of carbon fibre. It was a seldom occurrence to encounter intermittent printing issues - if there were any, they were usually not significant enough to cause major disruptions to the geometry of the printed square. Figure 10a shows a printed square of RA-013-2A' without glycol - this print has the distinctive coffee ring around it's perimeter, as expected. As the glycol concentration increases, it is noticed that the carbon fibre particles become more evenly distributed. Upon visual inspection, the sample in figure 10c of 10.1% glycol concentration shows the most consistent distribution of carbon fibre among the samples in figure 16. From 15.1% glycol onward, the distribution becomes less consistent. Surprisingly, figure 10e shows evidence of carbon fibre agglomeration which contributes towards the inconsistent distribution, even in the presence of glycol which is a surfactant-like compound.
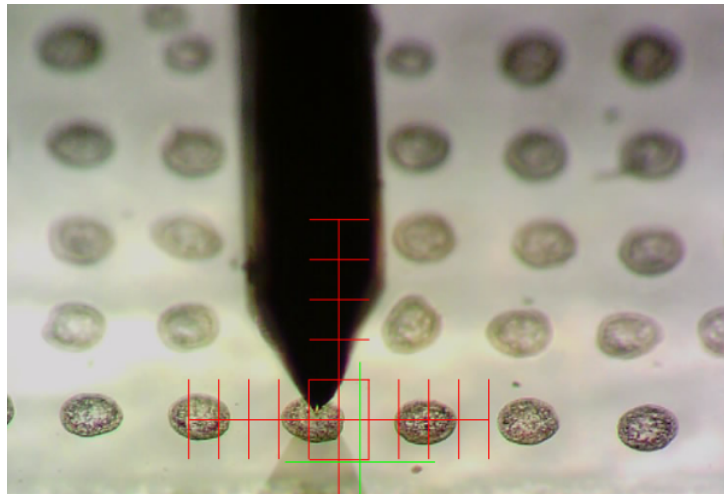
Figure 11   DektakXT profiler scanning individual RA-013-2A' 0% glycol droplets

(a) 0%   **(b)** 5.13%   **(c)** 10.1%

(d) 15.1%   **(e)** 20%   **(f)** 25.2%
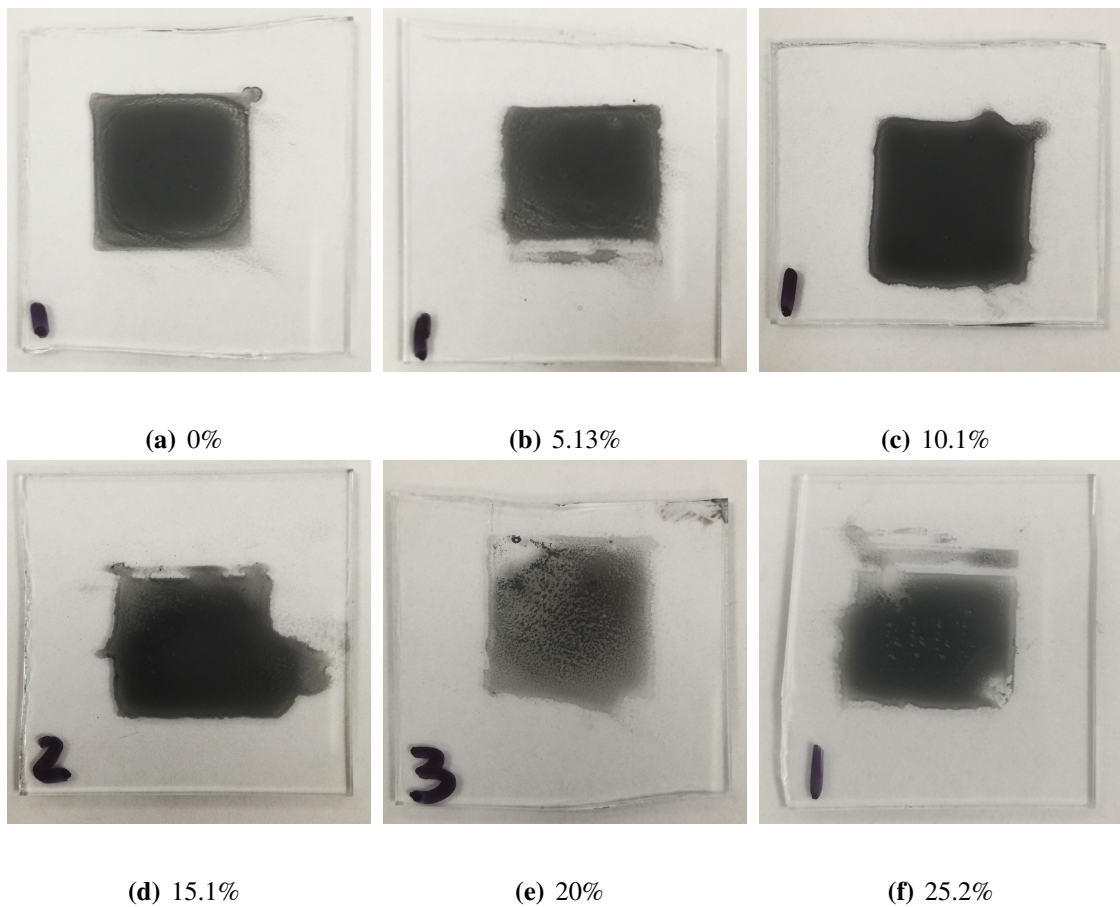
Figure 10   RA-013-2A' Square Prints at 500Hz with various Glycol Concentrations

2.5 Volume Profile

Visual inspection is limited by subjectivity and bound by its qualitative nature. To precisely and accurately quantify the effect glycol has on the coffee ring structures in the prints, a Bruker DektakXT surface profiling machine was used to characterise the cross section height of each ink glycol solution.
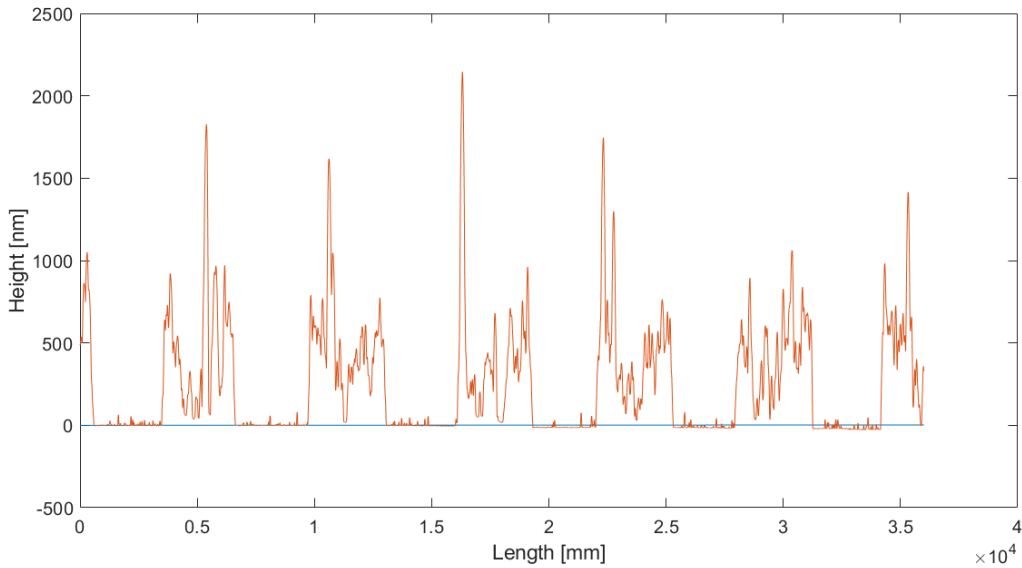
Figure 12   One out of three scans performed on RA-013-2A 0% glycol.

Sample	0.00g		
Scan Num.	1	2	3
Number of Droplets in Scan	5	5	5
Left Edge Height (nm)	1123	1094	724
Right Edge Height (nm)	688.5	813.7	763.8
Centre Height (nm)	209.9	1052	489.2
Nominal Edge Height (nm)	905.75	953.85	743.9
Edge:Center Height Ratio	4.315150071	0.906701521	1.520645953
Average Sample Ratio	2.247499182		

Table 4   Edge:Center Height ratio's calculated across multiple droplets within a single scan.

2.5.1   Method

To investigate each ink glycol solution, it is important that glycol's effect on individual droplets is observed. The printer was set to print at 30Hz, so that every droplet would isolated from one another. The surface profiler's stylus was run over 3 different rows of droplets for every ink glycol 30Hz printed sample. In total, there are 18 different scans. Five complete individual droplets of RA-013-2A 0% glycol, can be seen in figure 12. To quantify the coffee ring effect, a MATLAB script was run (see appendix A1) that crops each individual droplet from a scan and overlays them on top of one another. It then finds the average droplet profile over all the droplets in that specific scan. With the average scan profile, the nominal edge height to centre height was observed as a ratio so that the entire scan's average characteristic droplet shape can be recorded as a numerical value. An example of these values for RA-013-2A' 0% glycol are shown in table 5.

These ratio values are compared against every other glycerol sample to see the effect of glycerol concentration on this ratio, which is proportionately representative to the prevalence of the coffee ring effect.

Every sample's edge:center height ratio, other than the 0% glycol sample, remained around 1 ± 0.24. It appears that glycol, at all concentrations, reduces the edge:center ratio. Other than this, there does not appear to be any trend regarding glycol concentration and edge:center ratio.
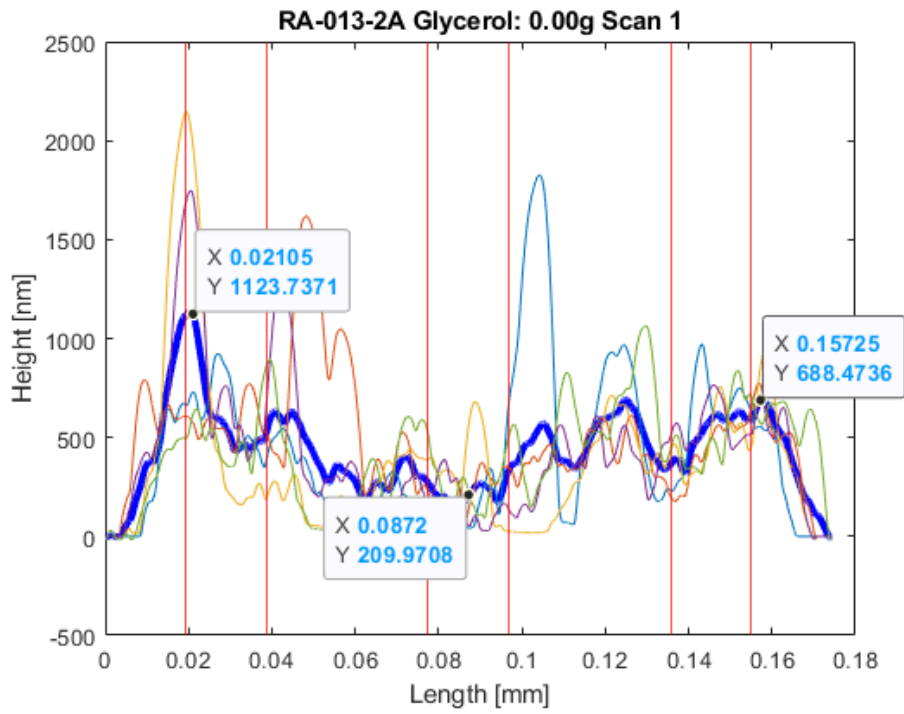
Figure 13　One out of three Average Profiles using RA-013-2A 0% glycol.

Glycol Concentration (%)	0.00	5.13	10.09	15.06	20.00	25.21
Ratio	2.25	0.91	0.98	1.15	0.76	0.87

Table 5　Table of sample edge:height ratios of RA-013-2A'.
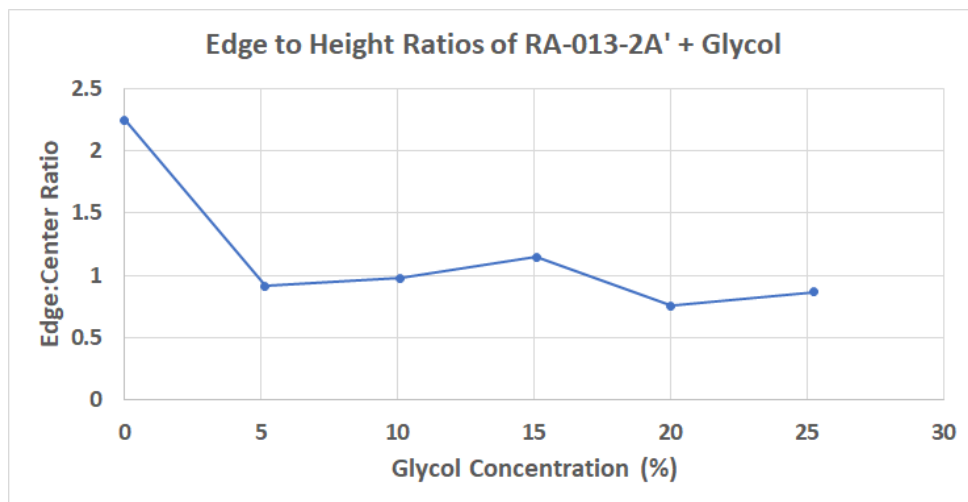
Figure 14　Graph of sample edge:height ratios of RA-013-2A'.

(a) 0%   **(b)** 5.13%   **(c)** 15.1%

(d) 20%   **(e)** 25.21%
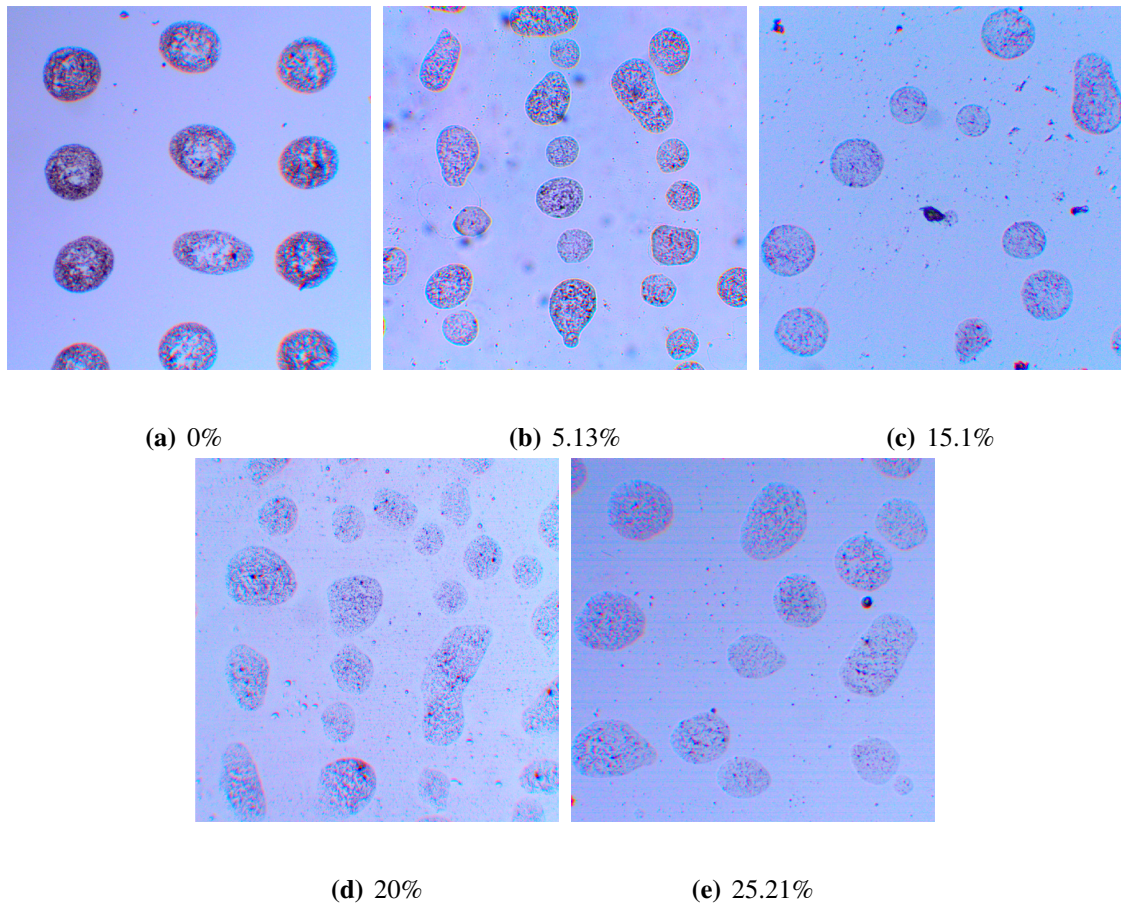
Figure 15 RA-013-2A' Square Prints at 30Hz with various Glycol Concentrations.

2.5.2 Method Inaccuracy

There lies an inherent inaccuracy within the method of ratio calculation. This inaccuracy arises when two droplets of the same scan that vary in diameter are overlapped on top of one another. This variation in diameter may be due to the alignment of surface profiler stylus travel direction, which was aligned by hand. This variation may also be caused by droplets following a non-straight path to the substrate when it is dispensed by the printer. These factors in combination contribute to the magnitude in variation. However, within a single scan, the droplets within that scan are generally of similar diameter. Droplets are less similar in diameter when compared to droplets of another scan for that sample. This is especially true for droplets with lower glycol concentrations.

Originally, ratios were calculated using the edge:center ratio of an average profile taken over all 3 scans for that sample. Using table 4 as an example, the average profile was taken over 15 different droplets across 3 different scans. The calculation procedure was then modified so that 3 separate average profiles are created, representative of the droplets within each scan, rather than 1 average profile to reduce the aforementioned inaccuracies.

Upon visual inspection using a microscope, it appears that out of all the samples in figure 15, the 0% glycol sample in figure 15a is the most ordered with respect to the grid-like pattern in which it was dispensed. It also appears that the orderliness of the dispensed pattern is inversely proportional to the glycol concentration.

On closer inspection, the structure of the droplet in figure 16a as observed through a microscope appears to show signs of the coffee ring effect - there is an agglomeration of

(a) 0% **(b)** 5.13% **(c)** 10.09%

(d) 15.1% **(e)** 20% **(f)** 25.21%
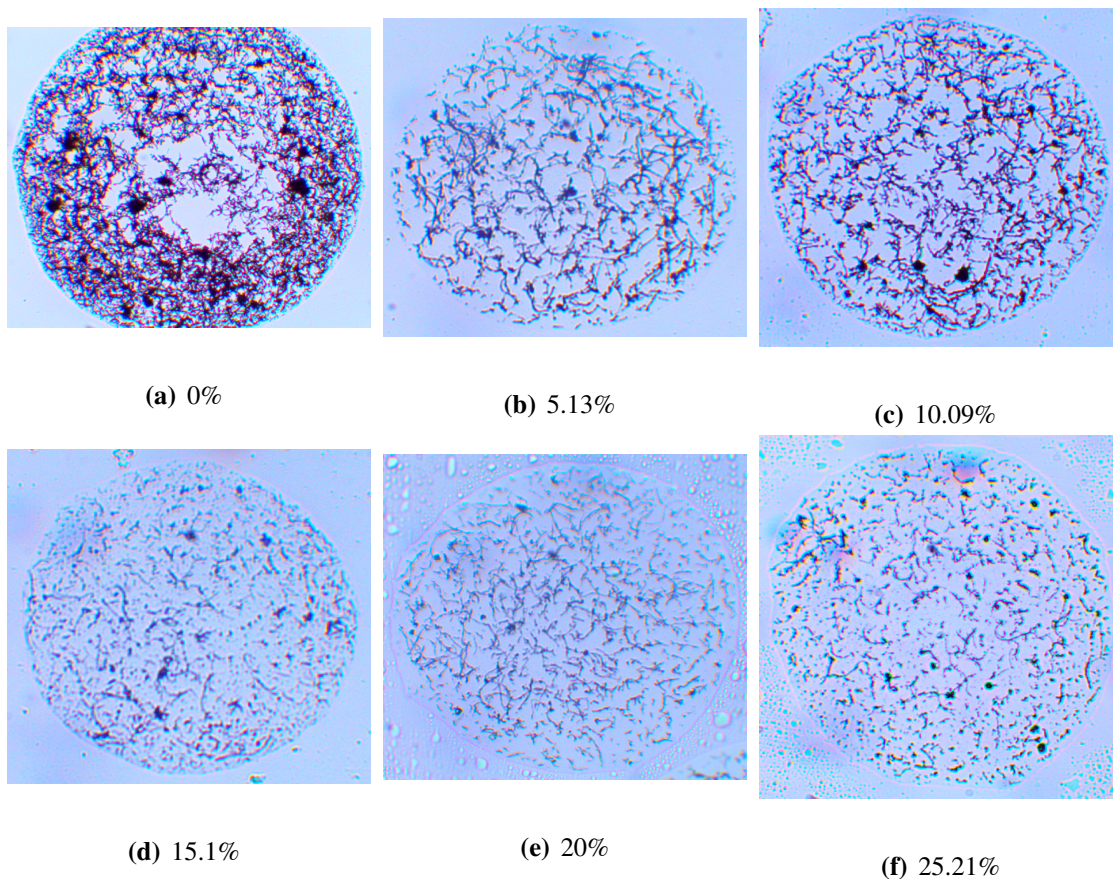
Figure 16 Close-up view of RA-013-2A' Square Prints at 30Hz with various Glycol Concentrations.

fibres around the edge of the circular droplet and there is less in the center. The individual carbon fibres start to become visible at this level. However, the image of the 10.09% glycol sample in figure 16c show no obvious signs of coffee ring effect. This confirms the respective edge:center ratio value (0.98) as both edges and center are very similar in height.

2.6 Viscosity

To gain further insight into the shelf life and particle dispersion, viscosity tests were conducted for various ink solutions after modifications had been made to their formulations.

2.6.1 *Before and after surfactant and glycol*

Before Triton X-100 and glycol was added to RA-013-3A as described in section 2.4.2, a viscosity test was conducted on the solution so that there was a baseline reading to compare against once the fluid was modified. Prior to testing, the fluid had be sonicated in a water bath for 30 minutes. Since the fluid is water-based, it is expected to behave as a Newtonian fluid - it is also expected that there will be a linear relationship between shear stress and shear rate. Surprisingly, the viscosity test showed a non linear, non symmetrical relationship, as shown in figure 17, for the first half of the test, even after sonication. In the second half of the test, the fluid followed a linear trend, as expected. The unusual behaviour in the beginning of the test suggests that the carbon fibres in the fluid had agglomerated and the viscosity test itself had aided in the mechanical dispersion of the fibres - this is why the second half of the test is linear. This would also suggest that RA-013-3A without additives has a very short shelf life.
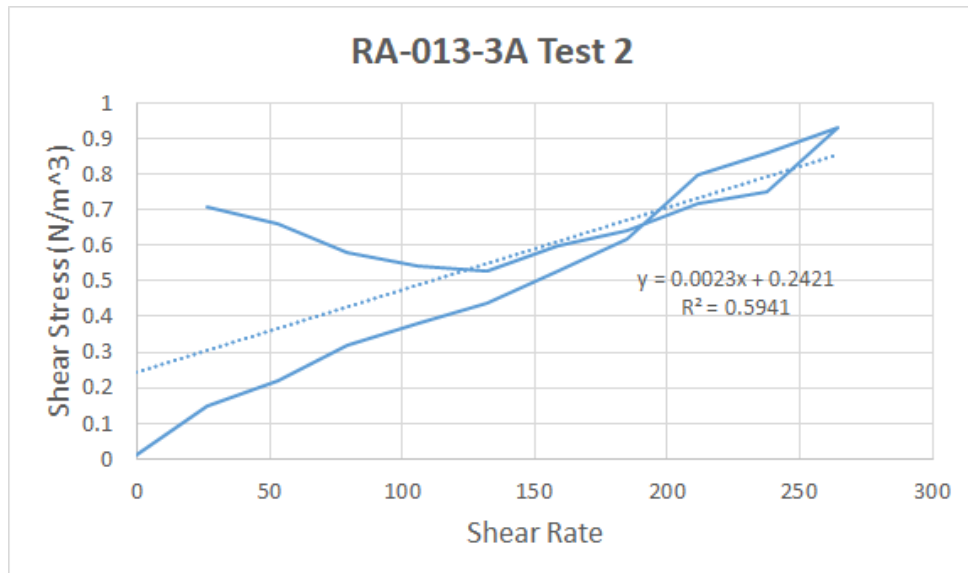
Figure 17   Viscosity test on RA-013-3A (no additives).

Step Num.	1	2	3	4	5	6	7	8	9	10	11	12	13	14	15	16	17	18	19	20
Speed (RPM)	20	40	60	80	100	120	140	160	180	200	180	160	140	120	100	80	60	40	20	0
Shear Stress (N/m^2)	0.71	0.66	0.58	0.54	0.53	0.6	0.64	0.72	0.75	0.93	0.86	0.8	0.62	0.53	0.44	0.38	0.32	0.22	0.15	0.01
Shear Rate	26.4	52.8	79.2	105.6	132	158.4	184.8	211.2	237.6	264	237.6	211.2	184.8	158.4	132	105.6	79.2	52.8	26.4	0

Table 6   Viscosity test on RA-013-3A (no additives).

2.6.2 Stability

Triton X-100 and glycol was then added to the RA-013-3A solution as described in section 2.4.2. A viscosity test was conducted on this solution to compare the effects of surfactant on viscosity and shelf life. The results are much more pleasing and a lot more Newtonian-like compared to that of the previous. The test is shows an improvement on the short-term shelf life and dispersion of the carbon fibres. Qualitatively expressed; the R^2 value changed from 0.59 to 0.99. The results can be seen in figure 18.

Following these results, the RA-013-3A solution with glycol and Triton X-100 was left in storage for 4 days. The viscosity was tested once again in the same fashion without
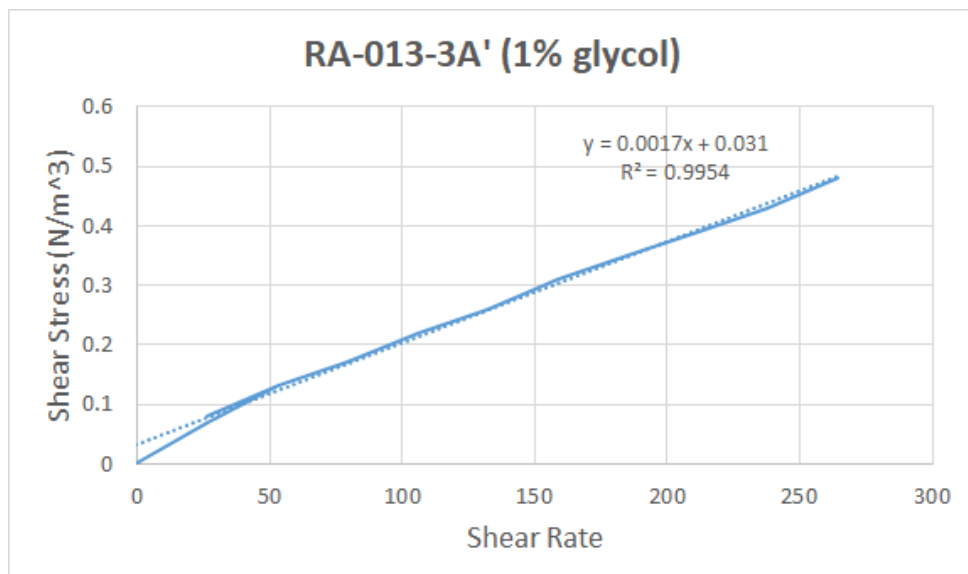
Figure 18   Viscosity test on RA-013-3A with glycol and Triton X-100.

14

Step Num.	1	2	3	4	5	6	7	8	9	10	11	12	13	14	15	16	17	18	19	20
Speed (RPM)	20	40	60	80	100	120	140	160	180	200	180	160	140	120	100	80	60	40	20	0
Shear Stress (N/m^2)	0.08	0.13	0.17	0.22	0.26	0.31	0.35	0.39	0.43	0.48	0.43	0.39	0.35	0.31	0.26	0.22	0.17	0.13	0.07	0
Shear Rate	26.4	52.8	79.2	105.6	132	158.4	184.8	211.2	237.6	264	237.6	211.2	184.8	158.4	132	105.6	79.2	52.8	26.4	0

Table 7   Viscosity test on RA-013-3A with glycol and Triton X-100.
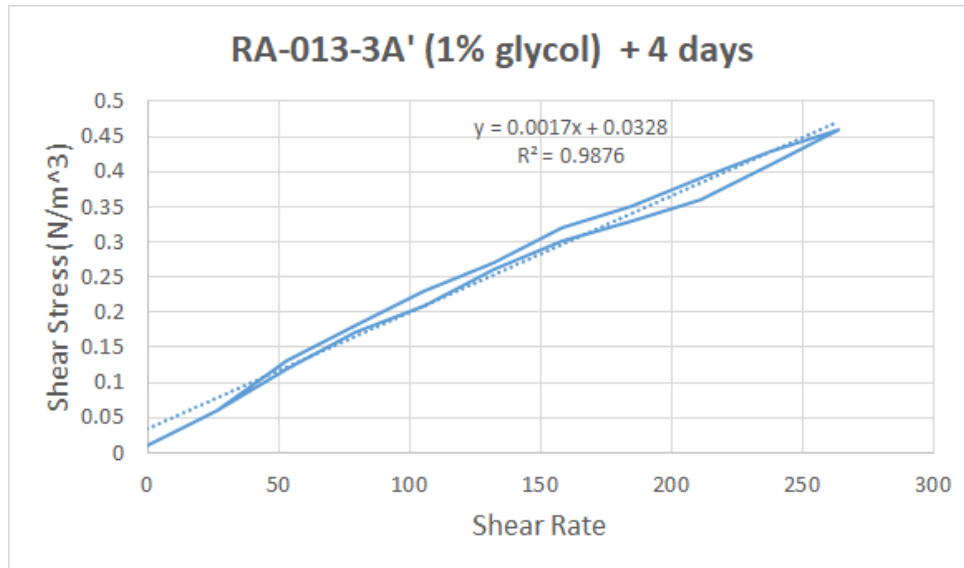
Figure 19   Viscosity test on RA-013-3A with glycol and Triton X-100 after 4 days.

sonication. The results can be seen in figure 19. The R^2 value did not change significantly and the gradient of the viscosity slope did not change. This means that the shelf life of the RA-013-3A solution with glycol and Triton X-100 is at least 4 days, which is a sufficient amount of time required for commercial inkjet operations.

2.7 Conductivity

2.7.1 Glycol's effect on resistance

Various square films were printed using RA-013-2A' and different glycol concentrations as seen in figure 16. The resistance of these films were inspected using a four point probe system and a Keysight B2902A precision measure unit, as seen in figure 20. Three samples were printed using each ink glycol solution. A resistance measurement was taken across each film sample at three different locations, totaling nine resistance measurements per ink glycol solution. The resistance of an ink glycol solution was found by taking the average across all nine resistance readings for that solution. The results are as shown in figure 21a and table 9.

It is observed that average resistance does not change significantly change between glycol concentrations of 0%, 5.13%, and 10.09%. However, between 10.09% and 15.06% glycol concentration, the resistance value jumps from 10.9kOhms to 72.5kOhms. This is most likely due to a decrease in concentration of carbon fibres throughout the film. This is not obvious when looking at figures 10c and 10d, however the decrease in carbon fibre concentration is visible when looking at a closer view in figures 16c and 16d. This trend continues as the glycol concentration increases.

Step Num.	1	2	3	4	5	6	7	8	9	10	11	12	13	14	15	16	17	18	19	20
Speed (RPM)	20	40	60	80	100	120	140	160	180	200	180	160	140	120	100	80	60	40	20	0
Shear Stress (N/m^2)	0.06	0.13	0.18	0.23	0.27	0.32	0.35	0.39	0.43	0.46	0.41	0.36	0.33	0.3	0.26	0.21	0.17	0.12	0.06	0.01
Shear Rate	26.4	52.8	79.2	105.6	132	158.4	184.8	211.2	237.6	264	237.6	211.2	184.8	158.4	132	105.6	79.2	52.8	26.4	0

Table 8   Viscosity test on RA-013-3A with glycol and Triton X-100 after 4 days.
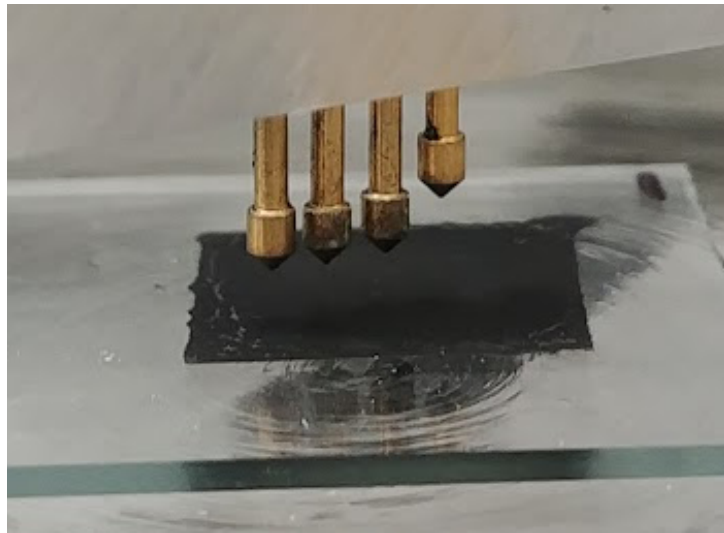
Figure 20 Four point probe and printed film.

No plasma oven treatment						
Glycol Concentration (%)	0.00	5.13	10.09	15.06	20.00	25.21
Average Resistance (kOhms)	1.708681444	3.665435444	10.90206144	72.51061667	180.3631444	234.6549889

Table 9 Average resistance values of RA-013-2A' films with various glycol concentrations.

2.7.2 Plasma Oven Treatment

The conductivity tested films was treated in a plasma oven to remove any impurities that may be increasing the resistance. Another conductivity test was conducted in the same aforementioned fashion. The results are shown in figure 21a and table 10. Having plasma oven treated the films, the resistances dropped considerably. Every average resistance value was now one ten thousandth of it's non plasma oven treated counterpart. The behaviour of the average resistance against glycol concentration curve in figure 21b is the same as that in figure 21a.

2.7.3 Effect of dwell time on resistivity.

Continuing the investigation into the effects of dwell time on the performance of the inks, a conductivity test was performed on the RA-013-3A films with glycol and Triton X-100, as described in section 2.4.2. These films are shown in figures 8 and 9. The results are displayed in tables 11 and 12. Reading from the tables 11 and 12, it appears that dwell time has a significant effect on the resistance of a film. The resistance of the untreated films after a dwell time of 4 days, on average is a factor of 330 times greater than that of the untreated films printed with no dwell time. The resistance of the plasma oven treated films after a dwell time of 4 days, on average is a factor of 345 times greater than that of the plasma oven treated films printed with no dwell time.

With plasma oven treatment						
Glycol Concentration (%)	0.00	5.13	10.09	15.06	20.00	25.21
Average Resistance (kOhms)	0.000170868	0.000366544	0.001090206	0.007251062	0.018036314	0.023465499

Table 10 Average resistance values of RA-013-2A' films with various glycol concentrations post plasma oven treatment.
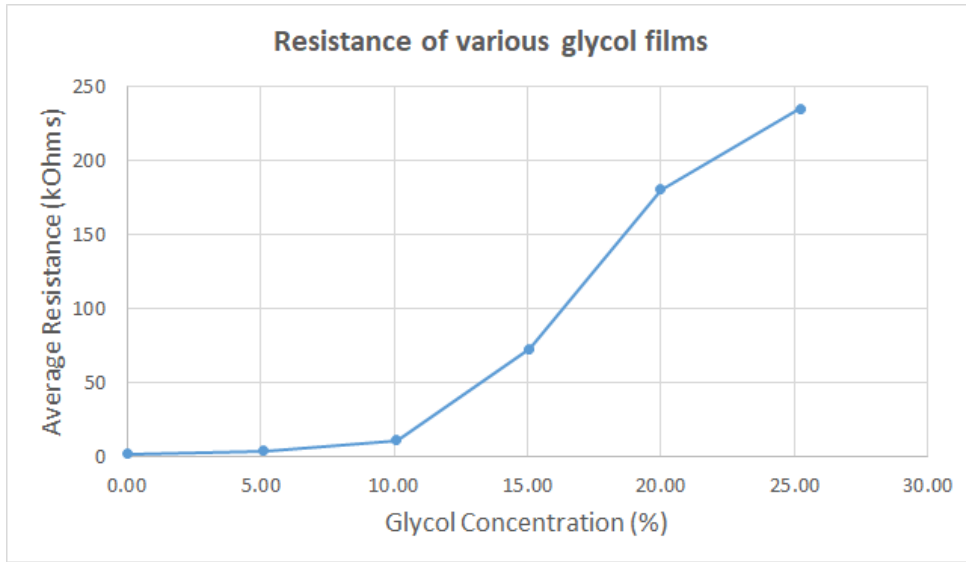
(a) Without plasma oven treatment.
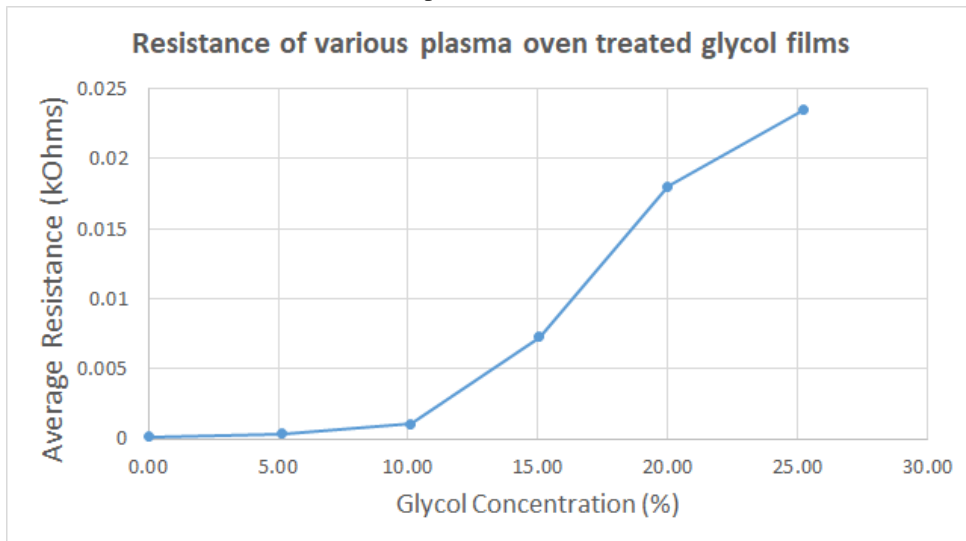
(b) With plasma oven treatment.

Figure 21   Average resistance values of RA-013-2A printed films with various glycol concentrations.

RA-013-3A with additives			
Sample Num.	1	2	3
Untreated	Average Sample Resistance (kOhms)	0.091790033	0.666623	1.09175
Plasma Oven Treated	Average Sample Resistance (kOhms)	9.179E-06	6.66623E-05	0.616721011

Table 11   Resistance values of RA-013-3A with additives with no dwell time.

RA-013-3A with additives + 4 days			
Sample Num.	1	2	3
Untreated	Average Sample Resistance (kOhms)	70.8696	83.18233333	100.892
Plasma Oven Treated	Average Sample Resistance (kOhms)	0.00708696	0.008318233	84.98131111

Table 12   Resistance values of RA-013-3A with additives with 4 days dwell time.

3. Discussion

Our experiments mainly investigated the fluid properties of the RA-013 formulations over the RA-011 formulations. RA-013 was chosen because they had lower viscosity values and therefore were more likely to print reliably. The RA-013 series of inks had no nanocellulose content, whereas the RA-011 series did. The difference in viscosity between the two ink series is likely due to presence of the nanocellulose. Carbon fibre agglomeration within the ink solutions was an ever-present occurrence throughout the study. This makes sonication necessary prior to printing any formulation. The detrimental effects of agglomeration were never circumvented, they were only reduced in significance.

In the first stages of this study, agglomeration was a significant hindrance in the production of printed films. So much so that in trying to print films using RA-013-1A', it became unusable after having reduced its water content in the process.

In the first stability test using RA-013-3A, it became apparent that surfactant Triton X-100 does have an effect on the dispersion of carbon fibre, however this effect was not able to be maintained over time due to print head blockages caused by agglomeration. After days of dwell time, this solution did print with less blockage interruptions, but this was attributed to a lower carbon fibre content in the printing reservoir as sedimentation had occurred in the ink storage containers.

Glycol concentration was then investigated for it's effect on the prevalence of the coffee ring phenomena in RA-013-2A' Square Prints. Visually, the 10.1% glycol concentration solution provided the most appealing results as the colour distribution was consistent throughout the shape. To gain an accurate and precise understanding of glycol's effect on these solutions, a surface profiling machine was used on individual droplets from samples of various glycol concentrations. As expected, the solution with no glycol content had the highest edge:center height ratio, whereas those with glycol had lower, but similar ratios. The solution that produced droplets with ratios closest to the ideal ratio of 1:1 was the 10.1% glycol concentration solution, with a ratio of 0.98:1. This confirms the subjective visual analysis of the previously mentioned colour distribution using this solution as accurate. Although there was inherent error in the way the ratios were calculated, the method was altered to reduce the significance of this problem.

Using a microscope, it again became visually apparent that across all RA-013-2A solutions with different glycol concentrations, the individual droplet with the least prevalence of coffee ring effect was the 10.1% glycol concentration solution.

The effect of dwell time on the viscosity of the RA-013-3A' solution was investigated. It's clear that without adding glycol or Triton X-100 to the working solution, carbon fibre will agglomerate within a short space of time, regardless of prior sonication. The strange behaviour in the viscosity test graph provides supporting evidence for this claim. However, adding glycol and Triton X-100 helped the working solution to maintain carbon fibre dispersion over a 4 day dwell time. Agglomeration was not evident using the data produced by the rheometer in this case. This, however is not an accurate assumption as the first dwell time experiment visually proves.

Conductivity tests were carried out on 18 different printed samples using RA-013-2A' with varying glycol concentrations. Data produced by a four point probe machine shows that the least resistive sample is produced by the working solution without any glycol. The resistance remains relatively low for samples produced containing 5.13% and 10.09% glycol. Samples with glycol concentrations higher than 10.09% produced samples with significantly higher resistance values. All samples were then treated for impurities in a plasma oven. The

resistance curves compared to that of the untreated samples were the same shape, however, all of the resistance values had dropped by a factor of 10,000, significantly reducing the resistance.

The effect on dwell time on resistivity was also investigated using RA-013-3A with glycol and Triton X-100 additives. After 4 days of dwell time, the RA-013-3A solution produced samples that had resistance values 330 times higher than that of the samples with no dwell time. This provides further supporting evidence for sedimentation in the storage container.

4. Further Work

If further investigation is to be conducted on the printability and final electrical performance of these inks, it is recommended that the method used to calculate the average droplet profile and thus edge:center ratio be modified so that the diameter of each droplet used in the average will not have a detrimental effect on the average profile as discussed.

The solution with the greatest printability and final electrical performance appears to be RA-013-2A' with 10.09% glycol concentration. It is recommended that solutions with glycol concentrations close to 10.09% should be investigated to provide a more precise insight as to the optimal glycol concentration for printability and electrical performance.

The RA-013 series of inks produced the most favourable viscosity values. It is recommended that more RA-013 solutions should be made with more finite increments of protein concentration to provide a more precise insight as to the optimal protein concentration for printability and electrical performance.

References

[1] S. Caizzone, C. Occhiuzzi, and G. Marrocco, "Multi-chip rfid antenna integrating shape-memory alloys for detection of thermal thresholds," *IEEE Transactions on Antennas and Propagation*, vol. 59, no. 7, pp. 2488–2494, 2011.

[2] H. Sirringhaus, T. Kawase, R. Friend, T. Shimoda, M. Inbasekaran, W. Wu, and E. Woo, "High-resolution inkjet printing of all-polymer transistor circuits," *Science*, vol. 290, no. 5499, pp. 2123–2126, 2000.

[3] K. J. Allen, "Reel to real: Prospects for flexible displays," *Proceedings of the IEEE*, vol. 93, no. 8, pp. 1394–1399, 2005.

[4] H. Andersson, K. Hammarling, J. Sidén, A. Manuilskiy, T. Öhlund, and H.-E. Nilsson, "Modified eas tag used as a resistive sensor platform," *Electronics*, vol. 1, no. 2, pp. 32–46, 2012.

[5] H. Nishide and K. Oyaizu, "Toward flexible batteries," *Science*, vol. 319, no. 5864, pp. 737–738, 2008.

[6] H. Warren, R. D. Gately, H. N. Moffat *et al.*, "Conducting carbon nanofibre networks: dispersion optimisation, evaporative casting and direct writing," *RSC Advances*, vol. 3, no. 44, pp. 21 936–21 942, 2013.

[7] J.-W. Song, J. Kim, Y.-H. Yoon, B.-S. Choi, J.-H. Kim, and C.-S. Han, "Inkjet printing of single-walled carbon nanotubes and electrical characterization of the line pattern," *Nanotechnology*, vol. 19, no. 9, p. 095702, 2008.

[8] B. K. Lok, Y. M. Ng, Y. N. Liang, and X. Hu, "Inkjet printing of multi-walled carbon nanotube/polymer composite thin film for interconnection," *Journal of nanoscience and nanotechnology*, vol. 10, no. 7, pp. 4711–4715, 2010.

[9] S. Rana, R. Alagirusamy, and M. Joshi, "Effect of carbon nanofiber dispersion on the tensile properties of epoxy nanocomposites," *Journal of Composite Materials*, vol. 45, no. 21, pp. 2247–2256, 2011.

[10] A. Russo, B. Y. Ahn, J. J. Adams, E. B. Duoss, J. T. Bernhard, and J. A. Lewis, "Pen-on-paper flexible electronics," *Advanced materials*, vol. 23, no. 30, pp. 3426–3430, 2011.

[11] J. Boge, L. J. Sweetman, S. F. Ralph *et al.*, "The effect of preparation conditions and biopolymer dispersants on the properties of swnt buckypapers," *Journal of Materials Chemistry*, vol. 19, no. 48, pp. 9131–9140, 2009.

[12] K. Kordás, T. Mustonen, G. Tóth, H. Jantunen, M. Lajunen, C. Soldano, S. Talapatra, S. Kar, R. Vajtai, and P. M. Ajayan, "Inkjet printing of electrically conductive patterns of carbon nanotubes," *Small*, vol. 2, no. 8-9, pp. 1021–1025, 2006.

[13] W. Gindl-Altmutter, J. Köhnke, C. Unterweger, N. Gierlinger, J. Keckes, J. Zalesak, and O. J. Rojas, "Lignin-based multiwall carbon nanotubes," *Composites Part A: Applied Science and Manufacturing*, vol. 121, pp. 175–179, 2019.

[14] D. A. Baker and T. G. Rials, "Recent advances in low-cost carbon fiber manufacture from lignin," *Journal of Applied Polymer Science*, vol. 130, no. 2, pp. 713–728, 2013.

[15] L. Vaisman, H. D. Wagner, and G. Marom, "The role of surfactants in dispersion of carbon nanotubes," *Advances in colloid and interface science*, vol. 128, pp. 37–46, 2006.

[16] A. Shimoni, S. Azoubel, and S. Magdassi, "Inkjet printing of flexible high-performance carbon nanotube transparent conductive films by âcoffee ring effectâ," *Nanoscale*, vol. 6, no. 19, pp. 11 084–11 089, 2014.

[17] C. Seo, D. Jang, J. Chae, and S. Shin, "Altering the coffee-ring effect by adding a surfactant-like viscous polymer solution," *Scientific reports*, vol. 7, no. 1, p. 500, 2017.

[18] R. Nagarajan and C.-C. Wang, "Theory of surfactant aggregation in water/ethylene glycol mixed solvents," *Langmuir*, vol. 16, no. 12, pp. 5242–5251, 2000.

Appendix A   Computer Code

Program A1   Mean Droplet Profile Generator MATLAB script

```matlab
1  %Title: Mean Droplet Profile Generator
2  %Author: Devdass Krishnan
3  %HOW TO SET UP PREREQUISITE DATA:
4
5  %For the case of RA-013-2a 0.25g:
6  %Import .csv file "RA-013-2a 0.25g 30Hz (1)" as a Numeric Matrix and
      rename
7  %it to "A".
8
9  %Import the .csv file with the Row Start and Row End columns and 4 more
10 %adjacent empty columns.
11
12 numberOfDroplets = size(dropletPositions,1);
13
14 widthDifference = zeros(numberOfDroplets, 1);
15 middleCell = zeros(numberOfDroplets, 1);
16 newRowStart = zeros(numberOfDroplets, 1);
17 newRowEnd = zeros(numberOfDroplets, 1);
18
19 %Finding the middle cell of all the droplets
20 for i = 1:numberOfDroplets %height of droplet matrix
21     differenceValueTemp = dropletPositions(i,2) - dropletPositions(i,1);
22     dropletPositions(i,3) = differenceValueTemp;
23     middleValueTemp = dropletPositions(i,1) + (differenceValueTemp/2);
24     dropletPositions(i,4) = middleValueTemp;
25 end
26
27 largestDifference = max(dropletPositions(:,3));
28
29 %Assigns new start and end points for the droplets using the
30 %largestDifference. This is so that each droplet dataset is the same
      width
31 %so we can add datasets together to find the average.
32 %This also makes sure that all droplets are aligned through their centre
      .
33 for i = 1:numberOfDroplets
34     middleValueTemp = dropletPositions(i,4);
35     newRowStartTemp = ceil(middleValueTemp - (largestDifference/2));
36     newRowEndTemp = newRowStartTemp + largestDifference;
37     dropletPositions(i,5) = newRowStartTemp;
38     dropletPositions(i,6) = newRowEndTemp;
39 end
40
41 %Locate droplets
42 %column 1: x position
43 %column 2: y height
44 drop1 = A((dropletPositions(1,5):dropletPositions(1,6)),(1:2));
45 drop2 = A((dropletPositions(2,5):dropletPositions(2,6)),(1:2));
46 drop3 = A((dropletPositions(3,5):dropletPositions(3,6)),(1:2));
47 drop4 = A((dropletPositions(4,5):dropletPositions(4,6)),(1:2));
48 drop5 = A((dropletPositions(5,5):dropletPositions(5,6)),(1:2));
49
50 %Add all the droplets to a single matrix to make operations easier
51 largeDropletMatrix = [drop1, drop2, drop3, drop4, drop5];%, drop6, drop7
      , drop8, drop9, drop10, drop11, drop12, drop13, drop14, drop15];
52
```

```matlab
53    %On either side of each droplet , make height zero so that adjacent
          droplet
54    %data doesn't affect the average .
55    for k = 1:2:( numberOfDroplets *2)
56        dropletNumber = (k + 1)/2;
57        droplet = largeDropletMatrix (: ,(k:(k+1)));
58        %left side of drop
59        for i = 1:( dropletPositions ( dropletNumber ,1) - dropletPositions (
              dropletNumber ,5) - 1)
60            if dropletPositions ( dropletNumber ,1) ~= dropletPositions (
                  dropletNumber ,5)
61                largeDropletMatrix (i ,(k+1)) = 0;
62            end
63        end
64        %right side of drop
65        for i = ( size ( droplet ,1) -( dropletPositions ( dropletNumber ,6) -
              dropletPositions ( dropletNumber ,2))): size ( droplet ,1)
66            if dropletPositions ( dropletNumber ,6) ~= dropletPositions (
                  dropletNumber ,2)
67                largeDropletMatrix (i ,(k+1)) = 0;
68            end
69        end
70    end
71
72    %Finding average droplet height over x axis .
73    %Add all the height values of each droplet together and divide by the
74    %number of droplets .
75    meanDroplet = zeros (( size ( largeDropletMatrix ,1)) ,2);
76    for k = 1:2:( numberOfDroplets *2)
77        meanDroplet = meanDroplet + largeDropletMatrix (: ,(k:(k+1)));
78    end
79    meanDroplet = meanDroplet /( size ( largeDropletMatrix ,2)/2);
80    meanDroplet2 = meanDroplet ;
81
82    i = largestDifference + 1;
83    j = 0;
84
85    %Resets all x axis data of droplets to range from 0 to the width of the
86    %largest droplet so that they can be overlapped .
87    for r = 1:i
88        for q = 1:2:( numberOfDroplets *2)
89            meanDroplet2 (r ,1) = j;
90            %Overlap all droplets
91            largeDropletMatrix (r ,q) = j;
92        end
93        j = j + 0.00005;
94    end
95
96    figure ;
97
98    x = meanDroplet2 (: ,1);
99    y = meanDroplet2 (: ,2);
100   p = plot (x,y, 'b');
101   title ('RA -013 -2A Glycerol : 1.25 g Scan 3');
102   xlabel ('Length [mm]')
103   ylabel ('Height [nm]')
104   p. LineWidth = 3;
105
106   hold on
107   y2 = largeDropletMatrix (: ,2);
```

```matlab
108  plot(x,y2)
109  y3 = largeDropletMatrix(:,4);
110  plot(x,y3)
111  y4 = largeDropletMatrix(:,6);
112  plot(x,y4)
113  y5 = largeDropletMatrix(:,8);
114  plot(x,y5)
115  y6 = largeDropletMatrix(:,10);
116  plot(x,y6)
117
118
119  meanDropletWidth = size(meanDroplet2,1);
120  sectorWidth = floor(meanDropletWidth/3);
121
122  xline(0.00005*(1/3)*sectorWidth,'r');
123  xline(0.00005*(1/3)*sectorWidth*2,'r');
124
125  xline(0.00005*(1/3)*sectorWidth*4,'r');
126  xline(0.00005*(1/3)*sectorWidth*5,'r');
127
128  xline(0.00005*(1/3)*sectorWidth*7,'r');
129  xline(0.00005*(1/3)*sectorWidth*8,'r');
130
131  sector1 = meanDroplet2(1:sectorWidth,:);
132  sector1max = max(sector1(:,2));
133  [rowmax1,colmax1] = find(sector1==sector1max);
134  sector1_x_pos = sector1(rowmax1, 1);
135  %plot(sector1_x_pos,sector1max,'r*');
136
137  sector2 = meanDroplet2(sectorWidth:sectorWidth*2,:);
138  sector2max = max(sector2(:,2));
139  [rowmax2,colmax2] = find(sector2==sector2max);
140  sector2_x_pos = sector2(rowmax2, 1);
141  %plot(sector2_x_pos,sector2max,'r*');
142
143  sector3 = meanDroplet2(sectorWidth*2:sectorWidth*3,:);
144  sector3max = max(sector3(:,2));
145  [rowmax3,colmax3] = find(sector3==sector3max);
146  sector3_x_pos = sector3(rowmax3, 1);
147  %plot(sector3_x_pos,sector3max,'r*');
148
149  hold off
```